CHAPTER 3

HIGH BIREFRINGENCE LATERALLY FLUORINATED TERPHENYL ISOTHIOCYANATES: STRUCTURAL, OPTICAL AND DYNAMICAL PROPERTIES

3.1 INTRODUCTION

Performance of a liquid crystal (LC) display device depends on the nature of the liquid crystalline material and the construction of the device. Fluoro substituted LC materials are found to be useful in large information content display devices. These are also promising materials for photonic applications because of their high birefringence [1−6]. Response time of a nematic liquid crystal (LC) based display device is proportional to rotational viscosity and square of the display cell thickness [7]. But reduced cell thickness (d) necessitates high birefringence material to attain the appropriate optical path given by Gooch–Tarry first minima condition (d. $\Delta n = \sqrt{3}\lambda/2$) in a twisted nematic cell [8]. Fast response time is especially important for color-sequential liquid crystal displays (LCDs) using blinking backlight [9] or primary-color (RGB) light emitting diodes (LEDs) [10]. In the RGB LED-backlit color-sequential LCDs, the pigment color filters can be eliminated, which not only reduces the LCD cost but also triples the device resolution. High Δn materials ($0.3 < \Delta n < 0.5$) are also useful in non-display applications like laser beam steering [11], tunable colour filters [12], focus tunable lens [13], electrically controlled phase shifter in GHz and THz region [14]. High birefringence also enhances the display brightness and contrast ratio of polymer-dispersed liquid crystals (PDLC), holographic PDLC, cholesteric LCD and LC gels [15–17]. In order to meet the demand for fast erelectro-optic response in nematic liquid crystal based display devices, new high birefringence (Δn) materials are, therefore, synthesized and their properties are studied in both pure and mixture state. The most effective method of increasing birefringence is to elongate the π-electron conjugation of the LC compounds by introducing multiple bonds or unsaturated (phenyl) rings in the rigid core structure. But highly conjugated liquid crystal compounds have the following problems viz; high melting temperature, increased viscosity, reduced UV stability and relatively low resistivity. The high melting temperature effect can be reduced through the lateral fluorination of the rigid core, which also hinders formation of smectic phases because of increased lateral force due to increased volume effect and lateral dipole moment (dipole moment of fluorobenzene is 1.50D) [18]. Although increased viscosity is inherent to all highly conjugated compounds, it can be mitigated by the proper choice of polar groups. UV stability can be improved by forming the rigid core of unsaturated rings instead of multiple bonds. The common rigid cores are phenyl, tolane and terphenyl structures and common polar groups are cyano (CN)

and isothiocyanato (NCS) which can serve the purpose. Moreover, due to lower dipole moment of NCS group (μ = 3.7 D) compared to CN group (μ = 3.9 D), viscosity of the NCS compounds is observed to be lower than the nitrile based systems [19]. This is thought to be due to formation of dimmers as a result of strong intermolecular interactions between the nitrile groups which is less probable in isothionato systems. However, a major concern of the CN- and NCS- based LC materials is their relatively low resistivity because of ion trapping near the polyimide alignment interfaces in device structure. Low resistivity leads to a low voltage holding ratio resulting in increased image flickering in thin film transistor (TFT) addressed liquid crystal displays. However, by fluorinating NCS compounds resistivity can be increased retaining high birefringence. Moreover, as mentioned, lateral fluorine substitution in the core also reduces the melting point substantially and hinders the formation of the smectic phases because of increased lateral force due to increased volume effect and lateral dipole moment.

In view of the above discussion three isothiocyanate terphenyl compounds with different lateral fluorine substitutions were selected for detailed investigation. In this chapter structural, optical and dynamical properties of those fluorinated compounds are reported and compared to see the effect of fluorination and chain flexibility. Eutectic mixtures of high birefringence nematogenic compounds are usually developed in order to satisfy various other physical properties including wide phase range, smectic compounds are also used in such mixture formulation [7,20,21]. In this respect the compounds under investigation are expected to be very useful in such mixture formulation. Other than positional ordering, reorientations of entire molecules around their short and long axes are one of the features that distinguish the liquid crystalline state from crystalline phase where these reorientations as well as intra-molecular reorientations are usually frozen, vibration of atoms about their equilibrium positions still persist. Therefore, information about the nature of molecular dynamics is possible to obtain from frequency and temperature dependent dielectric spectroscopic study. Although static dielectric data is available in the literature on some fluoro-substituted nematics, the authors are not aware of any report on their dielectric relaxation behavior.

3.2 COMPOUNDS STUDIED

Molecular structures of the investigated fluorinated terphenyl isothiocyanato compounds along with their abbreviated names and transition temperatures are given in the Table 3.1.

Table 3.1: Molecular structures and transition temperatures of 2TP-3'F-4NCS, 2TP-3',3F-4NCS and 4TP-3',3F-4NCS

Name	Molecular structure with transition temperature
2TP-3'F-4NCS	Cr **102.5ºC** SmA **120.5ºC** N **188.2ºC** I
2TP-3',3F-4NCS	Cr **80.2ºC** N **188ºC** I
4TP-3',3F-4NCS	Cr **58.1ºC** SmA **96.9ºC** N **181.8ºC** I
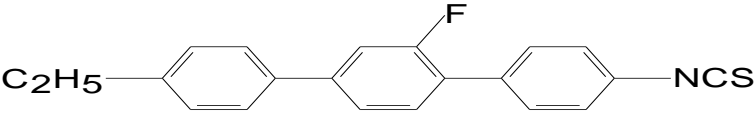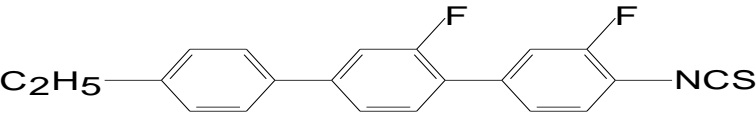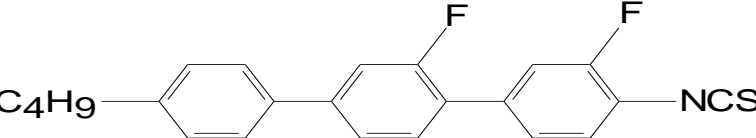
3.3 EXPERIMENTAL METHODS

The fluorinated terphenyl isothiocyanato compounds used in this investigation were supplied by Prof. R. Dabrowski, Military University of Technology, Warsaw, Poland. The phase behavior of the compounds was studied under an Olympus BX41 polarizing microscope regulating the temperature within ± 0.1ºC using Mettler FP 82 central processor and FP84 hot stage. Small and wide angle X-ray scattering measurements on randomly oriented samples were made using Ni filtered CuKα radiation and a custom built high temperature camera from ENRAF NONIUS FR590 X-Ray generator. X-ray photographs were scanned in 24 bit RGB colour format using HP2400C scanner. Optical densities of the pixels were calculated from the colour values and subsequently converted to X-ray intensities with the help of a calibration strip prepared by exposing the film for several known time intervals. Intensity distribution, obtained from the linear scan of X-ray photographs along the equatorial and meridional diffraction peaks, was used to determine average intermolecular distance (D) and apparent molecular length (l) in nematic phase or smectic layer spacing (d) with an accuracy of 0.02 Å and 0.1 Å respectively. The detailed procedures have been discussed in chapter 2 [22-25].

Static and frequency dependent dielectric properties have been studied using impedance analyzers HIOKI 3532-50 (50 Hz – 5 MHz) and HP 4192A (100 Hz –13 MHz), interfaced to a computer by RS-232 cable. Low resistivity (about 20 Ω/□) polyimide-coated homogeneous (HG) cells in the form of parallel plate capacitors with indium tin oxide (ITO) electrodes of ~ 3-5 μm cell gaps were used for static dielectric measurements. By applying sufficient DC bias field (~ 5V μm^{-1}) homeotropic (HT) alignment of the molecules was achieved in the same cell. Perpendicular and parallel components of the dielectric constants were obtained from capacitive measurements in HG and HT cells respectively as described in chapter 2. On the other hand, custom-built gold cells of thickness ~19 μm were used for frequency dependent complex dielectric permittivity measurements. In both cases, the cells were filled by capillary action with samples in isotropic state and cell temperature was maintained within ±0.1ºC using Eurotherm 2216e temperature controller. Very slow regulated cooling of the sample was made to get proper alignment.

Temperature dependent refractive indices were measured with He-Ne laser source (λ=633 nm) using Chatelain-Wedge principle. Thin prisms, with angles ~ 1º, were constructed using

optically flat glass slides rubbed with polyvinyl alcohol solution (1%) in such a way that the molecules are aligned with nematic director lying parallel to the edge of the wedge. Prisms were filled with samples in isotropic phase and cooled down very slowly. Further details of the measurement of refractive indices (n_o and n_e) have been described in chapter 2. The densities were measured at different temperatures using a dilatometer of capillary type which also has been described in chapter 2.

Molecules in the nematic phase have no positional correlation but they do have long-range orientational ordering. The extent of ordering is usually qualified by orientational order parameters (OOPs), which are uniaxial and are expressed by a traceless symmetric tensor of rank 2. Many physical properties like optical birefringence, dielectric anisotropy, threshold voltage for switching, etc., which are important device parameters, depend upon the OOPs. Orientational order parameter $<P_2>$ was calculated using the principal molecular polarizabilities α_o and α_e, perpendicular and parallel to the direction of optic axis, following de Gennes relation [26] as described in chapter 2. From the measured refractive indices and density values, the principal polarizabilities were calculated following the method of Neugebauer [27] as detailed in chapter 2.

3.4 RESULTS AND DISCUSSIONS

This chapter basically deals with fluorinated terphenyl compounds with a polar isothiocyanate (NCS) terminal group. With the goal of achieving the highest possible birefringence (Δn) value while retaining a relatively low viscosity and suitable mesomorphic properties, two types of lateral fluorine substitutions were studied. The first two compounds (2TP-3'F-4NCS and 2TP-3',3F-4NCS) have the same chain length with a single difference of one extra laterally fluorine substitution in the core and the third one (4TP-3',3F-4NCS) differs from the first two in respect of the chain length having two more carbon atoms. In this section, different characteristics of the compounds will be examined and comparisons will be made based on their structures and effect of fluorination.

3.4.1 Optical Polarization Microscopy

Observed textures, which are topological defect structures seen under optical microscope in crossed polarizers, confirmed the presence of different liquid crystalline phases and the transition temperatures for the above compounds. Typical textures have been obtained for all the phases of the three compounds. Observed focal conic texture in SmA phase and schlieren texture in nematic phase of 2TP-3'F-4NCS are shown in the Figure 3.1 as representative example. It is observed that the singly fluorinated compound 2TP-3'F-4NCS exhibits both smectic and nematic phase. Introduction of another lateral fluorine atom in the core (2TP-3',3F-4NCS) results in sharp decrease of melting point and complete suppression of smectic phase although clearing point remains same. In 4TP-3',3F-4NCS, where the terminal chain length is increased from 2 to 4 carbon atoms, the melting point is further reduced but SmA phase reappears. The smectic phase stability also increases in doubly fluorinated compound 4TP-3',3F-4NCS than the singly fluorinated compound 2TP-3'F-4NCS, being 38.8° and 18° respectively. All the three compounds possess nematic phase over a considerable temperature range – 68°C, 108°C and 85°C.
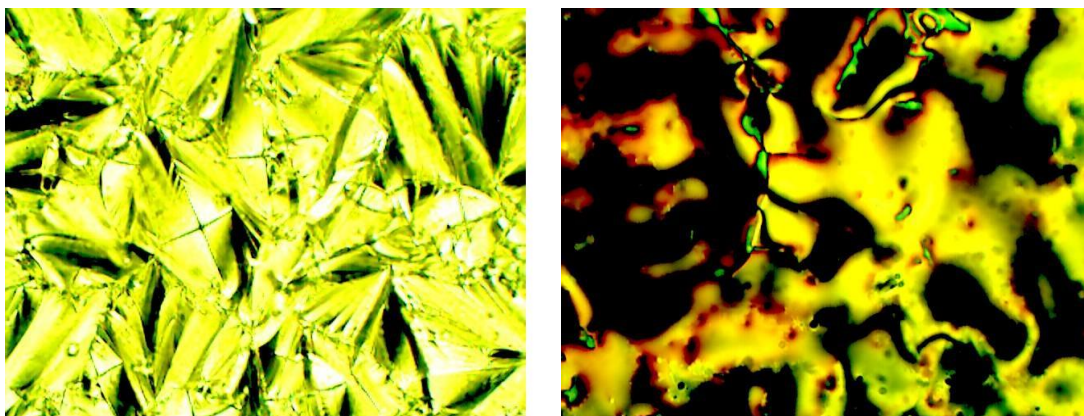
(SmA Phase 108°C)   (Nematic Phase 180°C)

Figure 3.1: Selected textures observed in 2TP-3'F-4NCS

3.4.2 Optimized Geometry Using Molecular Mechanics

To elucidate the structure of the investigated compounds, optimized geometry of the molecules were determined by molecular mechanics calculation using PM3 method in Hyperchem software package [28]. The optimized structures of the molecules, directions of the principal moments of inertia axes along with the direction of their electric dipole moments are shown in Figure 3.2. Values of optimized lengths of the molecules, dipole moments with the components along the three principal moments of inertia axes and the corresponding moments of inertia are shown in the Table 3.2.

Terphenyl core is found to be planar and the $-$ NCS group is almost in the same plane but not along the para axis of the core in all cases. At this point geometrical features of these molecules may be compared with those of an isothiocyanato compound 11CHBT for which crystal structural data are available [29]. Length of CN bond, by which the isothiocyanato group is connected to the phenyl ring, is found to be 1.41Å in all cases which is similar to that in 11CHBT (1.398Å). Observed NC and CS bond lengths are, in all cases, 1.24Å and 1.49Å. N-C-S bond angles are 172.9^o (2TP-3'F-4NCS), 171.9^o (2TP-3',3F-4NCS) and 172.8^o (4TP-3',3F-4NCS) which was 176.1^o in 11CHBT. The values of C-N-C bond by which the NCS group is connected to the phenyl ring are respectively 140.9^o, 142.1^o and 140.3^o which was 168.4^o in 11CHBT. Also C-N-N-S torsion angle is found to be almost 180° in all cases whereas that in 11CHBT was 167.3^o. Thus the conformation of the isothiocyanato phenyl group differs not only from that of 11CHBT molecule in the crystalline state but it is different in the three present molecules. As a result, dipole moment of 2TP-3'F-4NCS is found to be 5.57D, much larger than the dipole moment of the $-$ NCS group. This further increases to 6.68D in 2TP-3',3F-4NCS. However increase of chain length in 4TP-3',3F-4NCS does not increase the dipole moment rather it decreases slightly to 6.29D. Change of molecular conformation may be responsible for this.
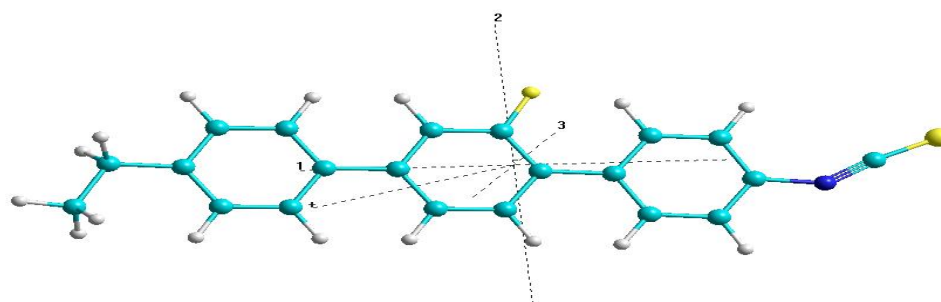
(a)
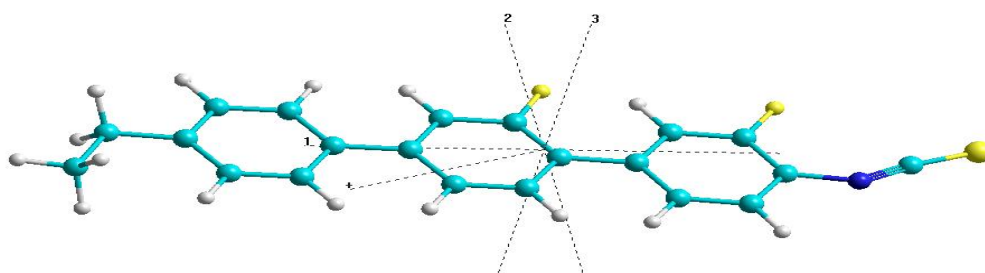
(b)
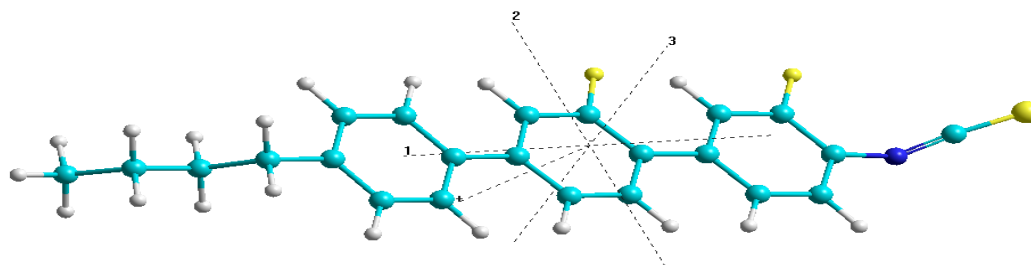
(c)

Figure 3.2: Optimized structure of the compounds (a) 2TP-3'F-4NCS, (b) 2TP-3',3F-4NCS and (c) 4TP-3',3F-4NCS

Molecular dipole moment is found to increase from 1.93D to 3.21D when in an axially fluorinated phenyl bicyclohexyl compound an additional lateral fluorine atom is added, but no change is observed when chain length is increased by two C-atoms (discussed in chapter 4). No change in dipole moment was reported in 1CB to 12CB molecules when measured by solution technique [30]. Such behavior was also observed in nCHBT series [31].

Table 3.2: Optimized length, dipole moment and moment of inertia

Compound	Optimized Length (Å)	Dipole Moment with components (Debye)	Moment of Inertia ($\times 10^{-46}$ kg m^2)		
			I_{XX}	I_{YY}	I_{ZZ}
2TP-3'F-4NCS	18.56	5.57 [5.48, 1.02, 0]	68.27	1471.02	1538.24
2TP-3',3F-4NCS	18.05	6.68 [6.39, 1.95, 0]	76.7	1550.0	1626.6
4TP-3',3F-4NCS	20.82	6.29 [5.83, 2.33, 0.41]	102.86	2048.83	2146.04

3.4.3 X-Ray Diffraction Study

X-ray diffraction photographs shows smectic and nematic phases clearly. The diffraction photographs contain two major diffraction maxima. Typical X ray diffraction photographs in SmA and nematic phases of the compounds are shown in Figures 3.3 – 3.5. Layer structure in SmA phase was clearly visible in the form of sharp inner ring compared to the nematic pattern. As discussed in chapter 2, the inner ring is related to the layer spacing (*d*) in the smectic phase and the apparent length of the molecule (*l*) in the nematic phase. The diffused outer ring arises

due to interaction of the neighboring molecules in a plane perpendicular to the molecular axis providing average intermolecular distance (**D**) [32].

<center>(a)</center>

<center>(b)</center>
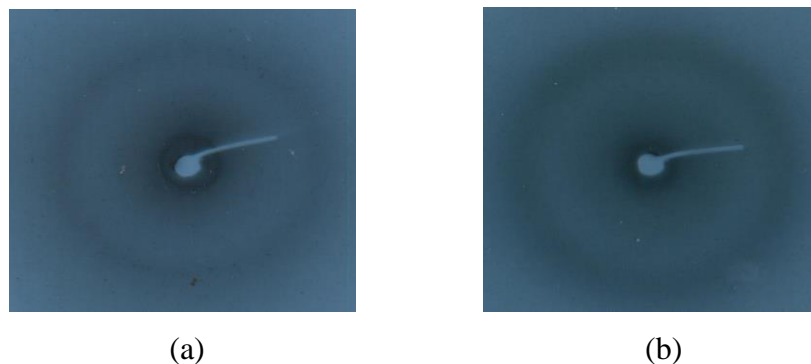
Figure 3.3: X-ray diffraction photographs in (a) SmA phase (110°C) and (b) nematic phase (125°C) of 2TP-3'F-4NCS

Figure 3.4: X-ray diffraction photographs in nematic phase (95°C) of 2TP-3',3F-4NCS

<center>(a)</center>

<center>(b)</center>
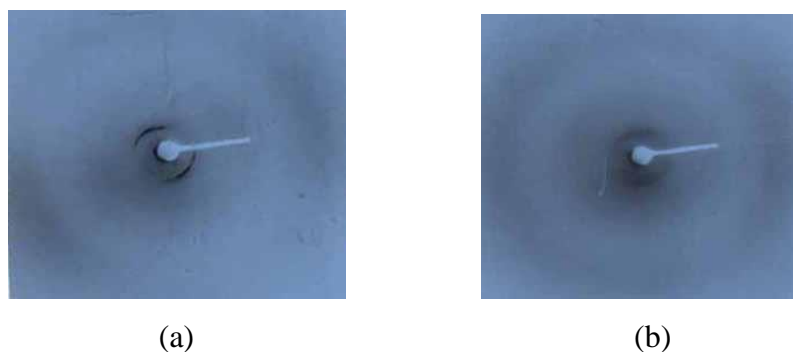
Figure 3.5: X-ray diffraction photographs in (a) SmA phase (60°C) and (b) nematic phase (100°C) of 4TP-3',3F-4NCS

Temperature dependence of the average intermolecular distance, apparent molecular length and smectic layer spacing are depicted in Figures 3.6 – 3.8 for the three compounds. It is evident that

D increases with temperature indicating a slight decrease in molecular packing. Average value of the intermolecular distances (D) in SmA phase is 5.03 Å which increases to 5.30 Å in nematic phase in 4TP-3',3F-4NCS. These values are considerably less than in singly fluorinated 2TP-3'F-4NCS; observed average values are 5.38 Å and 5.76 Å respectively. In doubly fluorinated 2TP-3',3F-4NCS also the average value is found to be 5.66 Å. It appears that increased flexibility in the chain results in more efficient packing of molecules in compound 4TP-3',3F-4NCS than the other two compounds. While comparing the compounds 2TP-3'F-4NCS and 2TP-3',3F-4NCS having the same chain length, D values are found to be slightly less in the singly fluorinated 2TP-3'F-4NCS compared to those observed in the doubly fluorinated 2TP-3',3F-4NCS. This is expected since introduction of additional F-atom in the core benzene ring increases lateral volume. This is further supported by the fact that in several homologues of non-fluorinated phenyl cyclohexyl based isothiocyanates D-values in nematic phase were found to vary from 5.06 to 5.12Å [33], much less compared to the fluorinated molecules. D was observed as 5.48 Å when one lateral fluorine atom was present in the benzene ring of a terminally fluorinated nematogenic bicyclohexyl phenyl compound, whereas it increased to 5.60Å when two lateral fluorine atoms were connected on opposite sides of the benzene ring [34]. Therefore, present observation on D is consistent with previous reported data of structurally similar compounds.
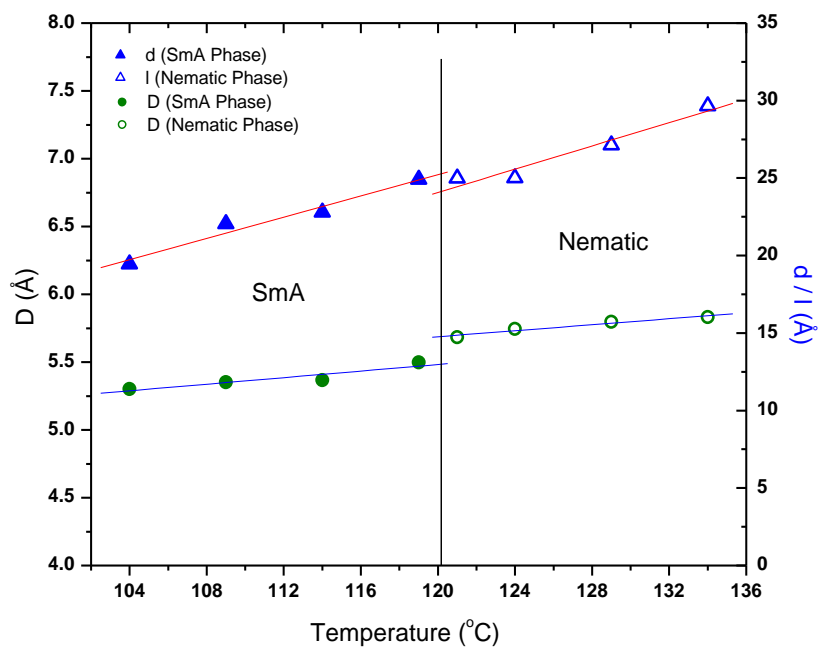
Figure 3.6: Temperature dependence of average intermolecular distance (*D*), smectic layer spacing (d) and apparent molecular length (*l*) of 2TP-3'F-4NCS
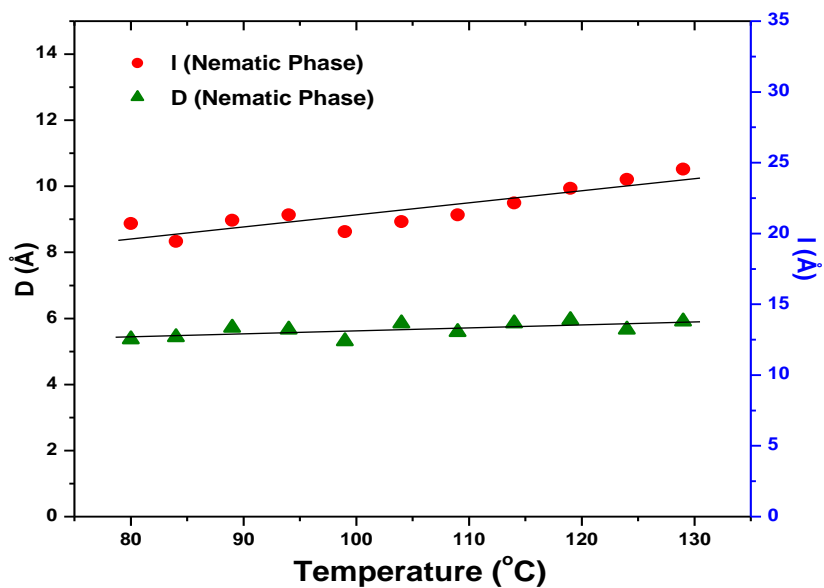
Figure 3.7: Temperature dependence of average intermolecular distance (*D*) and apparent molecular length (*l*) of 2TP-3',3F-4NCS
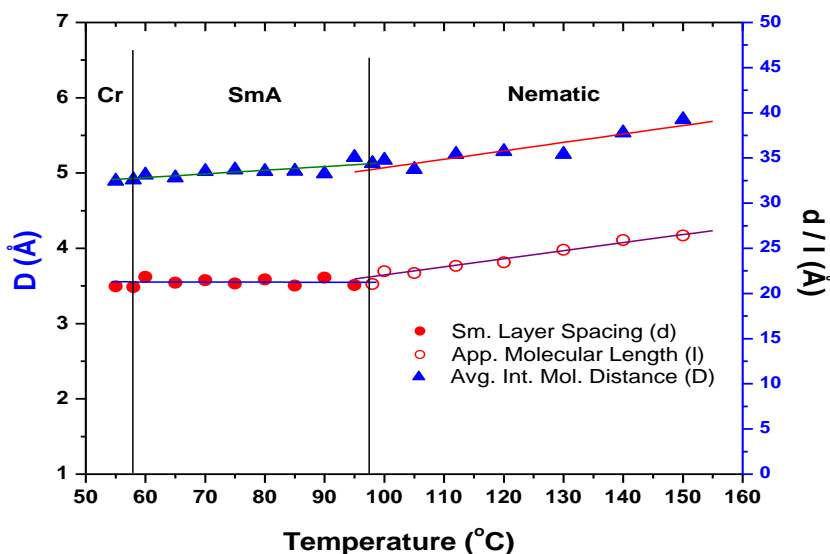
Figure 3.8: Temperature dependence of average intermolecular distance (*D*), smectic layer spacing (d) and apparent molecular length (*l*) of 4TP-3',3F-4NCS

In 2TP-3'F-4NCS and 4TP-3',3F-4NCS, the smectic layer spacing (d) is found to increase respectively from 19.45 Å to 22.78 Å and 20.7 Å to 21.0 Å, while effective length of the molecules (*l*) increases from 24.9 Å to 27.12 Å and 22.5 Å to 26.4 Å in the nematic phase as shown in Figure 3.6 and 3.8 respectively. However in 2TP-3',3F-4NCS which possess only nematic phase, the effective length of the molecules (*l*) is found to increase from 20.7 Å to 24.5 Å. Linearly fitted data show clear discontinuities at SmA-N transition in both the parameters D and *l*, more in 2TP-3'F-4NCS than in 4TP-3',3F-4NCS, signifying first order phase transition; although according to Mc Millan theory it should be second order in nature since observed T_{NA}/T_{NI} in both the cases is less than 0.87 [35,36]. Moreover, observed effective length of the molecules in N phase and layer spacing in smectic phase are slightly higher (more in less chained system) than the molecular length obtained from geometry optimization for all the three compounds. Similar behavior was also observed in non-fluorinated isothiocyanatobenzenes [37]. To explain this observation, some sort of molecular association among the neighboring molecules are considered, usually antiparallel molecular associations are suggested in molecules having terminal polar groups [38], no such association is observed in systems having no terminal polar groups from either X-ray study or dielectric study [39,40]. Crystal structure analysis on structurally similar terminally and laterally fluorinated pheny bicyclehexyl compounds also

revealed such type of associations [41,42]. Molecular mechanics calculations yielded the parallel and perpendicular component of dipole moments as 5.48D and 1.02D for the compound 2TP-3' F-4NCS which were 6.39D and 1.95D respectively in 2TP-3',3F-4NCS whereas in 4TP-3',3F-4NCS the values are 5.83D and 2.33D respectively. Thus, although the molecules are not strictly axially polar but axial dipole moments are much stronger than the transverse components resulting in antiparallel associations. In the homologues of non-fluorinated alkylcyclohexyl isothiocyanatobenzenes we observed l to vary from 1.04 to 1.16 at T=0.98T_{NI} [33]. Although dipole moments of the present compounds are much larger than that of alkylcyclohexyl isothiocyanatobenzenes, slightly less molecular overlap in the antiparallel dimeric association is observed in the present case compared to the non-fluorinated isothiocyanatobenzenes. This may be the result of increased steric interaction due to the presence of lateral fluorine atoms and shorter terminal chain. With increasing temperature thermal energy probably helps to overcome the dipolar interaction partially, thereby increasing the layer spacing and the apparent molecular length. Antiparallel molecular associations in NCS compounds were also confirmed from crystal structure analysis of the 11CHBBT, the 11th member of phenyl cyclohexyl isthiocyanates [43].

3.4.4 Static Dielectric Study

Dielectric Permittivities

Dielectric permittivity measurements were made at 10 kHz in planar (HG) cell. In order to determine switching voltage required to switch molecular alignment from planar (*HG*) to homeotropic (*HT*) configuration, dielectric permittivity was measured as a function of DC bias voltage across the cell. The switching characteristic in nematic phase is shown in Figure 3.9 for all the three compounds. Voltage at which the real part of dielectric permittivity increases by 10% from its minimum value is called threshold voltage (V_{th}) and at which it reaches 90% of the maximum value is termed as driving voltage (V_d). In 4TP-3',3F-4NCS threshold and driving voltages are found to be respectively 4.78V and 10.12V where as in 2TP-3' F-4NCS these are found to be 4.52 V and 9.6 V and for 2TP-3',3F-4NCS the corresponding values are 3.8V and 7.0V. Threshold and driving voltage increase slightly with chain length but decreases considerably with addition of another lateral fluorine atom. Thus increasing chain length has

more effect on switching of the molecules compared to increased lateral fluorination. However the combined effect of increased chain length and lateral fluorination is less than the effect of individual changes. However, driving field for all the compounds is suitable for thin ($< 2\mu$m) TFT based LC display cells. Nevertheless, $5\text{V}\mu\text{m}^{-1}$ field was used for switching from HG to HT configuration while measuring $\varepsilon_{\parallel}$.

(a)

(b)

(c)
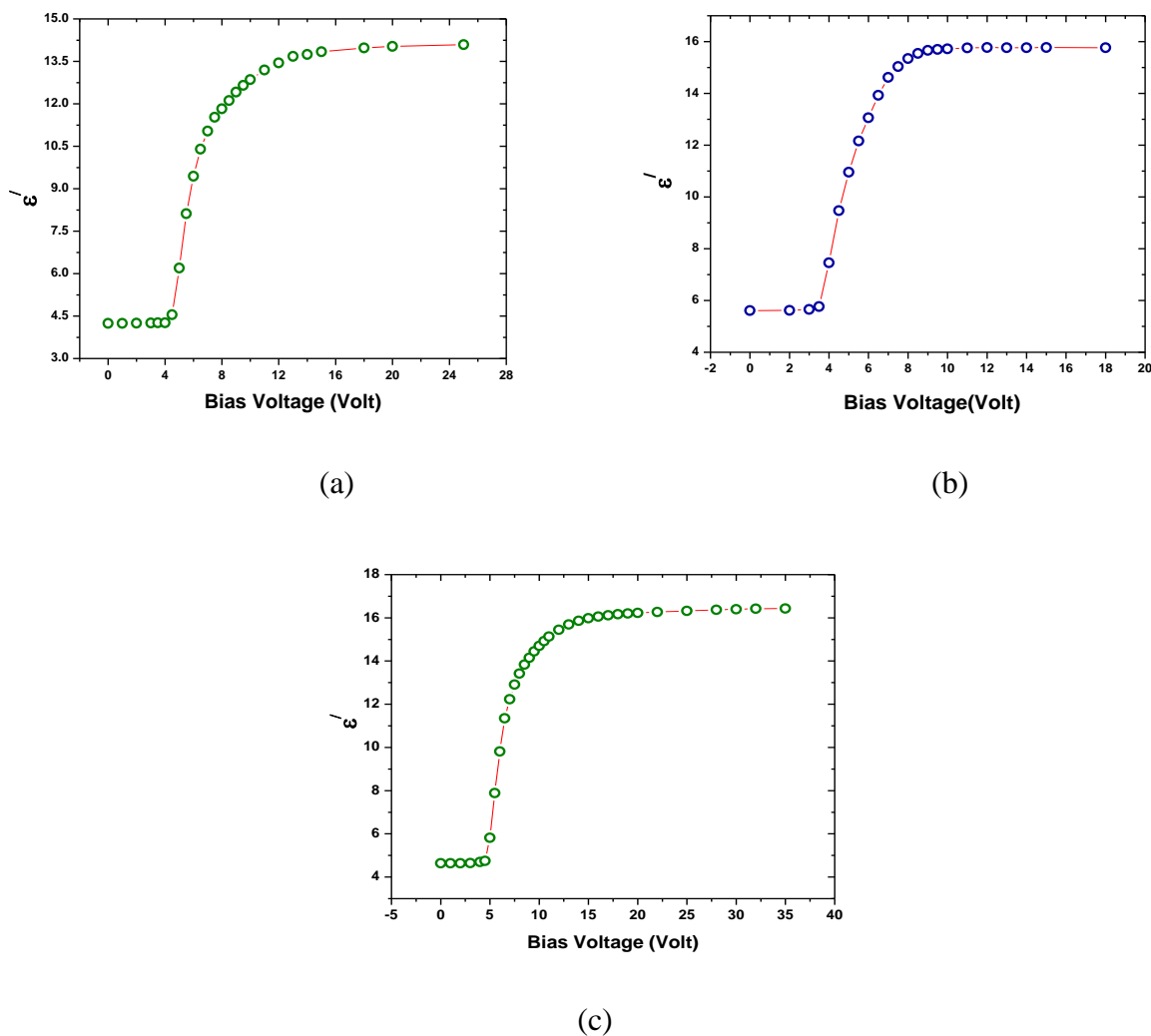
Figure 3.9: Real part of dielectric constant (ε') in nematic phase as a function of bias voltage at 10 kHz in ITO cell for (a) 2TP-3' F-4NCS, (b) 2TP-3',3F-4NCS and (c) 4TP-3',3F-4NCS.

Temperature variations of principal dielectric constants along and perpendicular to the molecular axis have been depicted in Figures 3.10 − 3.12. It is observed that in SmA phase $\varepsilon_{\parallel}$

decreases slowly with increasing temperature whereas $\varepsilon_\perp$ remains almost constant for the compounds 2TP-3' F-4NCS and 4TP-3',3F-4NCS. Slight discontinuity is observed in the dielectric parameters at SmA-N transition although not as prominent as observed in X-ray study. Average value of the dielectric constant ε_{av}, defined as $(\varepsilon_\| + 2\,\varepsilon_\perp)/3$, also remain almost independent of temperature. In nematic phase stronger temperature dependence of both the components are observed. Selected values are shown in the Table 3.3. Since the molecules possess quite strong axial dipole moment, $\varepsilon_\|$ is found to be large (about 17.4 near Cr-SmA transition) compared to $\varepsilon_\perp$ (about 4.3) whereas corresponding values are 17 and 6, and 14.9 and 3.9, respectively in the doubly and singly fluorinated homologues. Comparatively larger values in the former two compounds compared to the later is due to the fact that the dipole moments along and perpendicular to molecular axes are large in the former two compounds than in the latter as noted earlier.

   Temperature variations of dielectric anisotropy ($\Delta\varepsilon = \varepsilon_\| - \varepsilon_\perp$) for all the compounds are shown in Figure 3.13 for comparison. Dielectric anisotropy is found to decrease with temperature; decrement rate is, however, less in smectic than in nematic phase. $\Delta\varepsilon$ near Cr–N transition in 2TP-3',3F-4NCS is found to be 10.64 whereas in 2TP-3' F-4NCS observed $\Delta\varepsilon$ near Cr–SmA transition is 10.97 and near SmA-N transition it is 9.7. In 4TP-3',3F-4NCS the corresponding values are 13.02 and 12.2 respectively which is considerably higher than in the ethyl compounds. From the figure it is evident that with increased lateral fluorination $\Delta\varepsilon$ slightly decreases, but it increases when chain length is also increased by two carbon atoms. In a 4-propylphenylbicyclohexyl-3,4-difluorobenzene compound with two fluorine substituents at terminal position of the benzene ring (abbreviated as 3PBC^{3,4}F$_2$) maximum value of $\Delta\varepsilon$ was found to be about 6 [44], whereas in a 4,4'-propylterphenyl compound having the same alkyl chain at both ends but with two fluorine substituents at vicinal position of the central benzene ring it was about -1.2 [45]. Thus present observation on $\Delta\varepsilon$ is consistent with previous reports on structurally similar compounds.
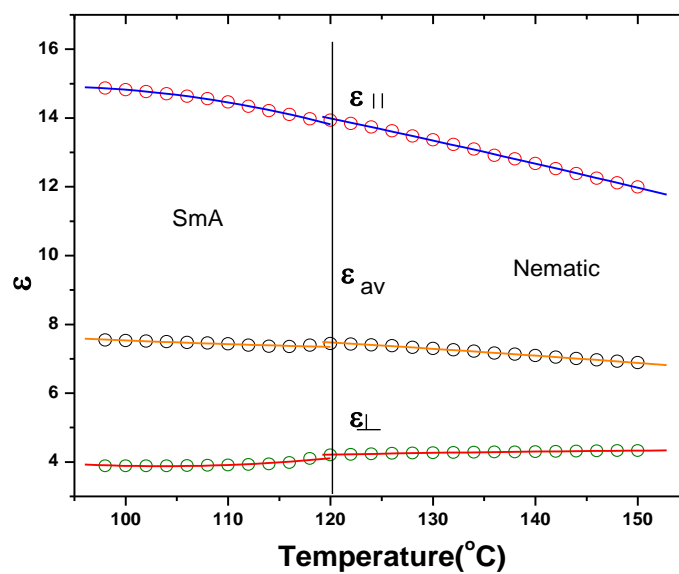
Figure 3.10: Variation of static dielectric constants as a function temperature at 10 KHz in ITO cell in 2TP-3'F-4NCS
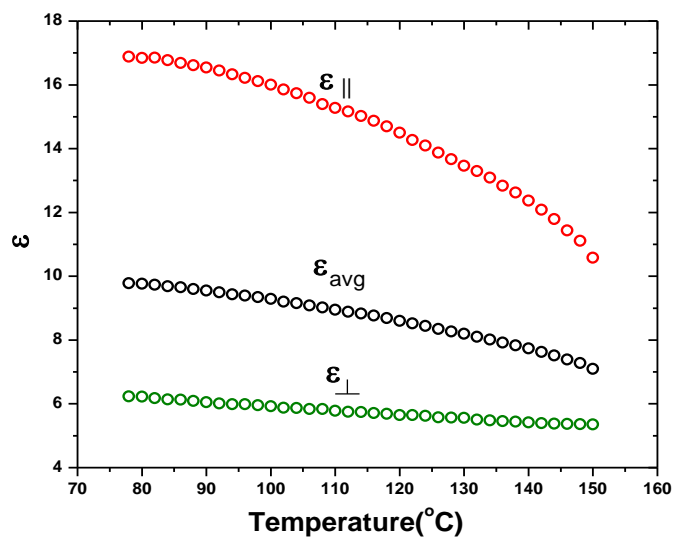
Figure 3.11: Variation of static dielectric constants as a function temperature at 10 KHz in ITO cell in 2TP-3',3F-4NCS
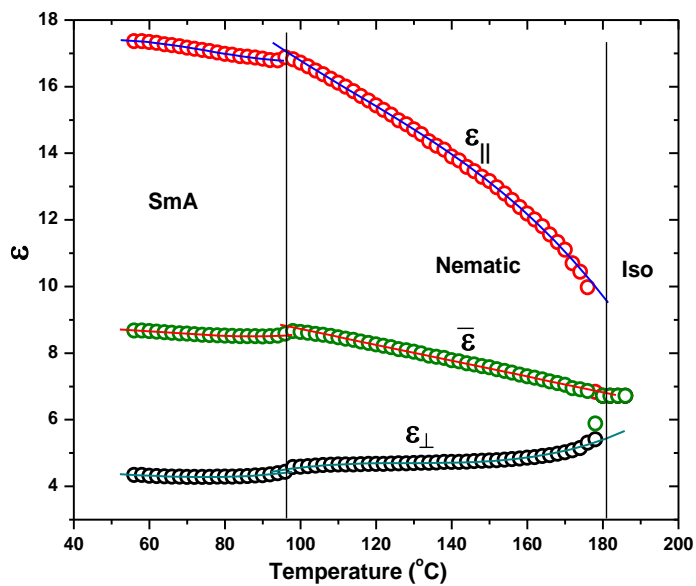
Figure 3.12: Variation of static dielectric constants as a function temperature at 10 KHz in ITO cell in 4TP-3',3F-4NCS
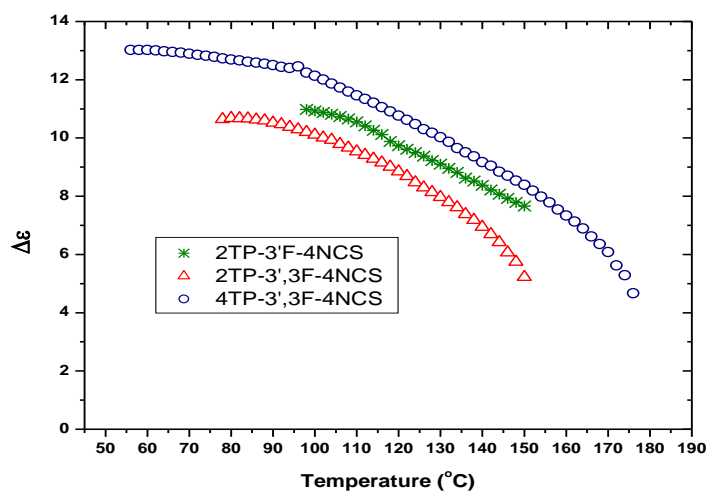
Figure 3.13: Temperature dependence of dielectric anisotropy of the compounds

Table 3.3: Selected static dielectric parameters of compounds

Compound	Threshold voltage (V_{th}) (V)	Driving voltage (V_d) (V)	$\varepsilon_{\parallel}$ (Near melting point)	$\varepsilon_{\perp}$ (Near melting point)	$\Delta\varepsilon$ (Near melting point)
2TP-3'F-4NCS	4.52	9.6	14.86	3.88	10.97
2TP-3',3F-4NCS	3.8	7.0	16.88	6.23	10.64
4TP-3',3F-4NCS	4.78	10.12	17.36	4.34	13.02

Dipole Correlation Factors

Effective values of dipole moments (μ_{eff}) were calculated following Bordewijk [46] theory of anisotropic dielectrics, as described in chapter 2. μ_{eff} was found to less in both smectic and nematic phases compared to free molecular dipole moments in all the compounds again suggesting antiparallel correlation of the neighbouring molecules. To obtain a quantitative measure of this correlation, dipole-dipole correlation factor g_λ, was calculated, as described in chapter 2. It is noted that $g_\lambda = 1$ signifies no correlation at all (monomeric system), $g_\lambda = 0$ means perfect antiparallel correlation and $g_\lambda = 2$ means perfect parallel correlation. Calculated values are shown in Table 3.4. In 2TP-3'F-4NCS, $g_{\parallel}$ is found to be 0.35 in smectic phase and 0.39 in nematic phase signifying weak antiparallel correlation of the components of dipole moments along the molecular axes in nematic phase, correlation slightly improves in smectic phase.

Table 3.4: Effective value of dipole moments (μ_{eff}) and dipole correlation factors (g_λ)

Compound	Temp (ºC)	μ_{eff} (D)	$g_\parallel$	$g_\perp$
2TP-3'F-4NCS	105	5.37 (SmA)	0.35	0.88
	110		0.37	0.85
	120		0.38	0.95
	125	5.40 (N)	0.39	0.96
	130		0.39	0.97
	140		0.40	0.95
	150		0.41	0.92
2TP-3',3F-4NCS	85	6.0 (N)	0.37	0.91
	90		0.37	0.92
	100		0.38	0.90
	110		0.37	0.88
	120		0.37	0.85
	130		0.36	0.80
	140		0.35	0.75
	150		0.31	0.70
4TP-3',3F-4NCS	60	6.05 (SmA)	0.38	0.52
	80		0.40	0.54
	100	6.36 (N)	0.44	0.62
	120		0.45	0.66
	140		0.48	0.66
	160		0.52	0.64
	180		0.55	0.67

Corresponding values of $g_\perp$ were 0.88 and 0.96 suggesting almost no antiparallel correlation of the perpendicular components of the dipole moments. Antiparallel correlations in both directions decrease further with temperature. In 2TP-3',3F-4NCS antiparallel correlation along the

molecular axis is slightly less ($g_{\parallel} = 0.37$) in nematic phase than in the singly fluorinated compound. g_{λ} values in 4TP-3',3F-4NCS suggests that slight increase of chain flexibility results in further decrease of antiparallel correlation along the molecular axis slightly but correlation increases substantially in the perpendicular direction. Although it was thought before that NCS compounds do not form dimers [21] like the CN compounds but X-ray study in the crystalline and liquid crystal phases as well as dielectric study in liquid crystal phases confirm antiparallel correlation of neighboring molecules. X-ray and dielectric study in the crystalline and mesomorphic phase in other NCS compounds also supports this observation [29,31].

Dielectric Relaxation Study

To see the dynamic response of the molecules to an ac field, frequency dependent dielectric study was performed as a function of temperature in a gold coated cell. The frequency dependences of dielectric permittivities (real and imaginary part) of the three compounds are shown in Figures 3.14 – 3.16. It is clear from the figures that the real part of dielectric permittivity remains almost constant in the low frequency region and decreases sharply at higher frequencies. As temperature increases real part of dielectric permittivity is found to decrease continuously in singly fluorinated 2TP-3'F-4NCS and doubly fluorinated 4TP-3',3F-4NCS. On the other hand, in the doubly fluorinated 2TP-3',3F-4NCS, initially it is found to increase slightly, then decreases although it contains only nematic phase. Different temperature dependence may be due to different phase behaviour. Considerable supercooling effect is observed and dielectric behaviour is slightly different in the supercooled state in the ethyl compounds.
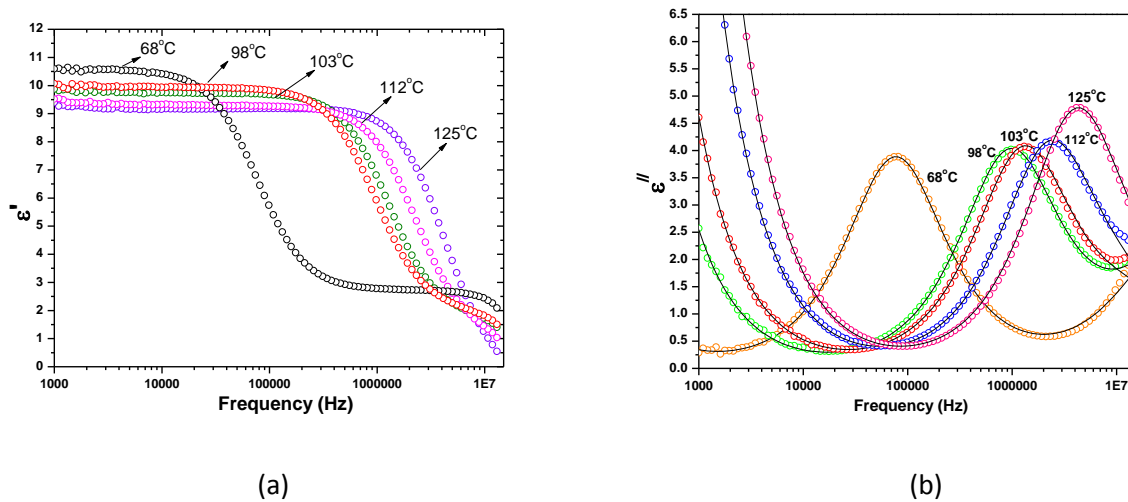
Figure 3.14: Dispersion (a) and absorption (b) spectra at some selected temperatures in 2TP-3'F-4NCS. Solid curves in (b) represent curves fitted to modified Cole-Cole function as described in text
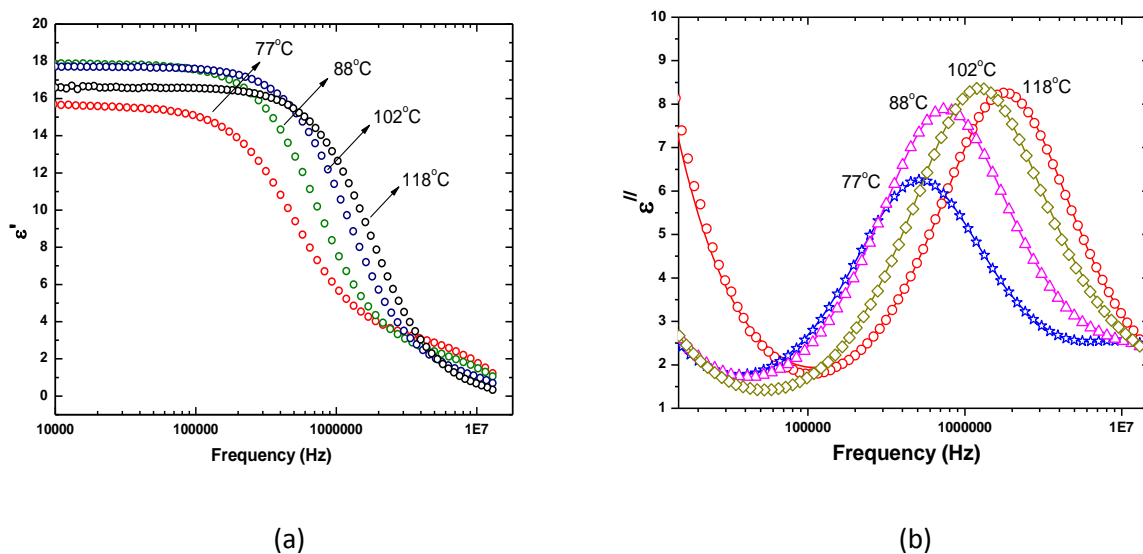
Figure 3.15: Dispersion (a) and absorption (b) spectra at some selected temperatures in 2TP-3',3F-4NCS. Solid curves in (b) represent curves fitted to modified Cole-Cole function as described in text
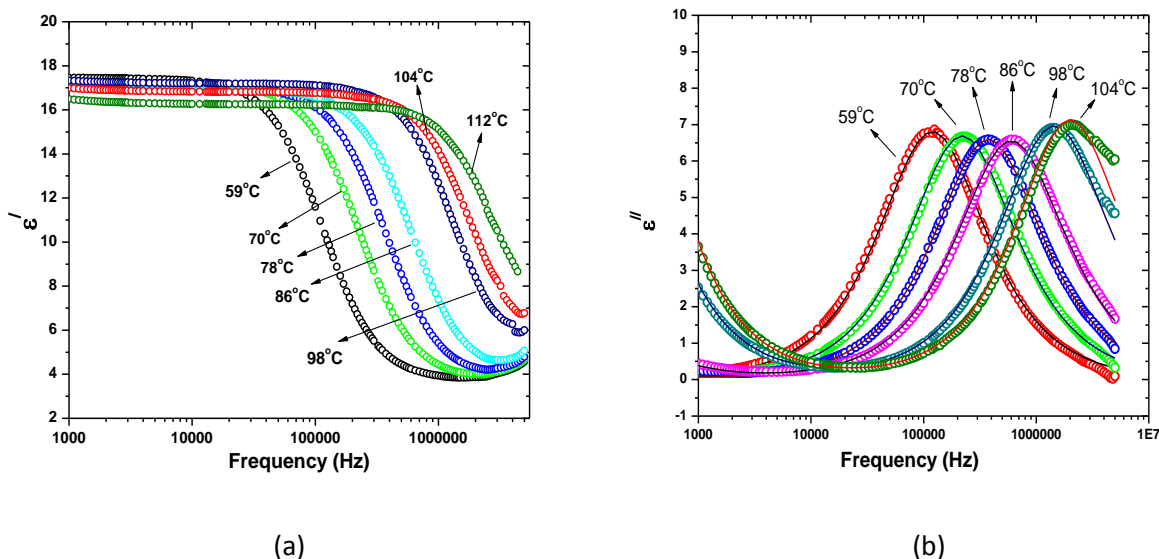
Figure 3.16: Dispersion (a) and absorption (b) spectra at some selected temperatures in 4TP-3',3F-4NCS. Solid curves in (b) represent curves fitted to modified Cole-Cole function as described in text

Only one strong absorption process is observed in dielectric spectra as evident from Figures 3.14(b), 3.15(b) and 3.16(b), for clarity spectra only at some selected temperatures are presented. The $\varepsilon^{//}$ peak height increases slightly with temperature in the smectic A as well as in the nematic phase in 2TP-3'F-4NCS and considerably in 2TP-3',3F-4NCS and thus there are a larger number of free molecules (monomers) with a corresponding enhancement of the effective dipole moment at higher temperature [47]. But in case of 4TP-3',3F-4NCS, there is no effective change in the $\varepsilon^{//}$ peak height with temperature implying no appreciable change in dipolar correlation at higher frequencies in this compound. However, in all the compounds relaxation frequencies are found to increase with temperature. Assuming the relaxation behavior is a result of Cole–Cole type process, the complex dielectric permittivity was fitted with the modified Cole-Cole equation [48] to get the actual values of relaxation frequency (*fc*) and symmetric distribution parameter (α), details have been described in chapter 2. As real and imaginary parts of dielectric constants are related through Kramers-Kronig relations, the Cole-Cole plot of the fitted spectra at a particular temperature for all the compounds are presented in Figure 3.17 –

3.19, which shows that the fitting was quite good. Nature of the absorption process is found to be almost Debye type since in no case fitted α is more than 0.05.
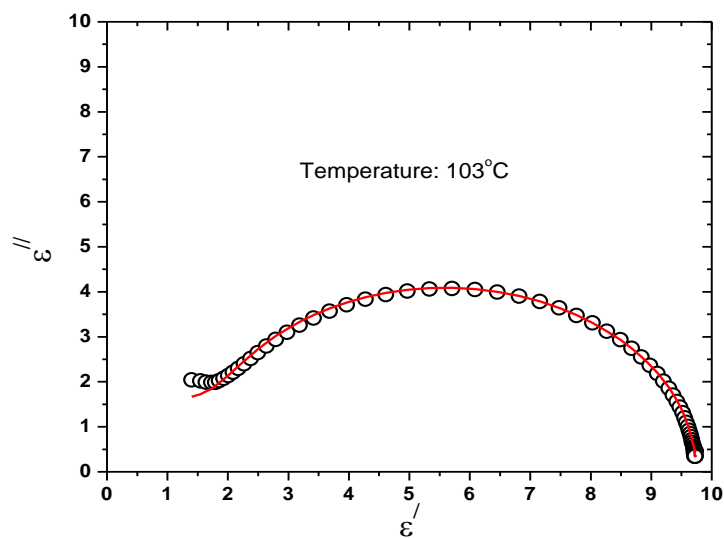
Figure 3.17: Cole-Cole plot of 2TP-3'F-4NCS
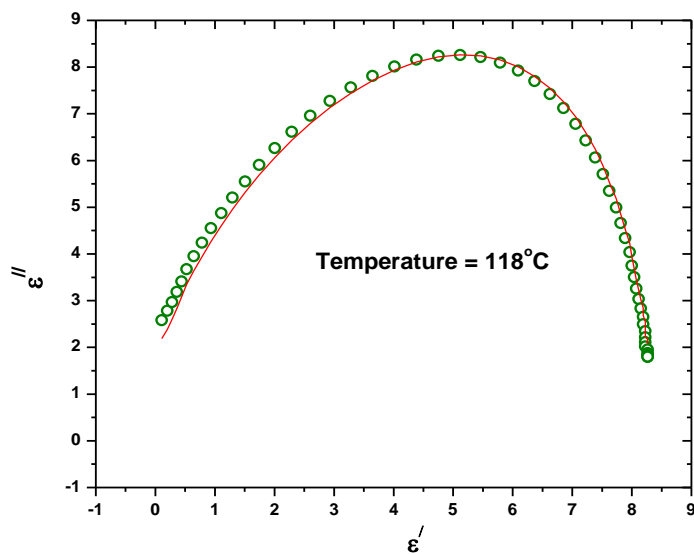
Figure 3.18: Cole-Cole of 2TP-3',3F-4NCS
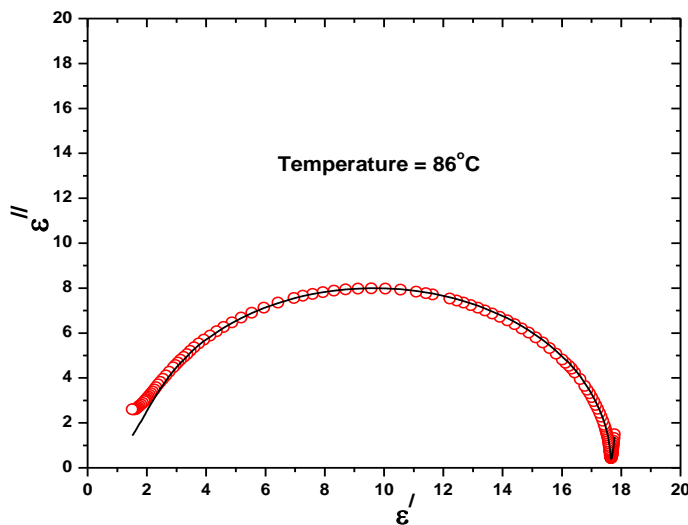
Figure 3.19: Cole-Cole plot of 4TP-3',3F-4NCS

Relaxation frequency, assumed to be associated with rotation around short molecular axis (flip-flop mode), increases systematically with temperature, shown in Table 3.5 and Figures 3.20 – 3.22. Critical frequency in nematic phase is found to decrease with increased fluorination and chain length, effect is more in the former case. In SmA phase opposite behavior is observed in low temperature region. In various smectic phases, however, critical frequencies were found to increase as the homologous series is ascended and was explained by introducing the idea of their dependence on anisotropic free volume [49,50].

Critical frequencies of the present compounds are lower than in cyanobiphenyls e.g. in 5CB it was 15.6 MHz [51]. This is expected since for rigid molecules critical frequency varies inversely with square root of moment of inertia [52] and the present molecules have larger moments of inertia (listed in Table 3.2) mainly because of large increase in their molecular mass compared to 5CB in which the moment of inertia was calculated from optimized geometry and found to be 42.9×10^{-46} kg m^2, 844.1×10^{-46} kg m^2, 884.3×10^{-46} kg m^2. In a structurally more closely related compound, propyl terphenyl isothiocyanatobenzene with fluorine atoms at 3,5 positions of isothiocyanato benzene group (which may be abbreviated as 3TP-3,5-4NCS), relaxation frequency was found to vary from 900 kHz to 4 MHz [53], closer to present observation.
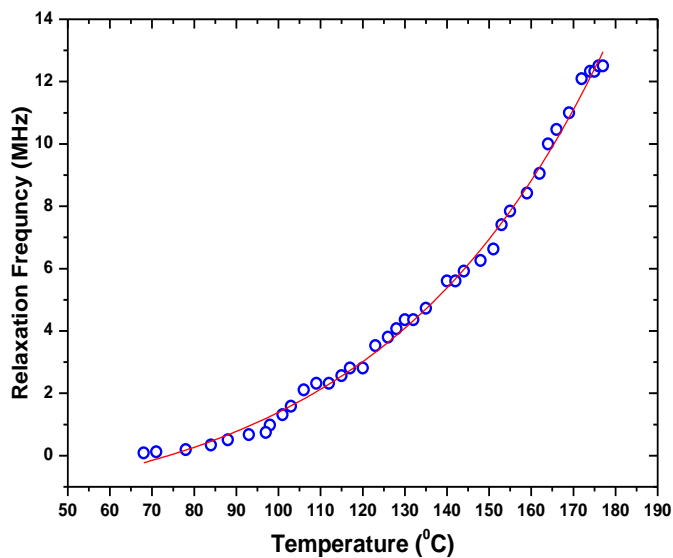
Figure 3.20: Temperature variation of relaxation frequency of compound 2TP-3'F-4NCS
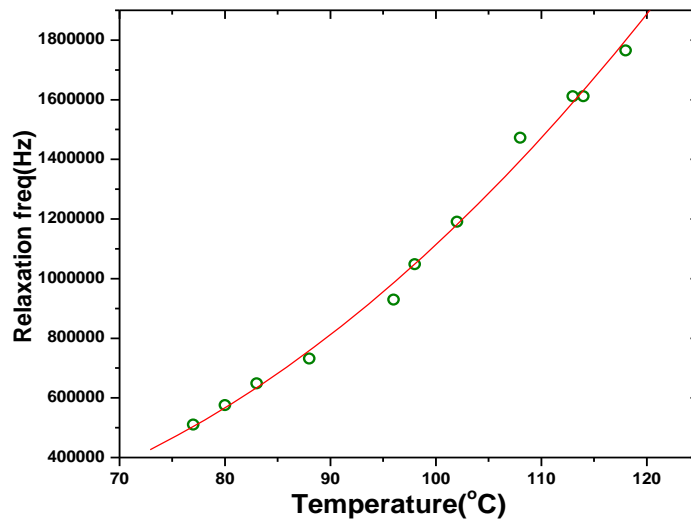
Figure 3.21: Temperature variation of relaxation frequency of compound 2TP-3',3F-4NCS
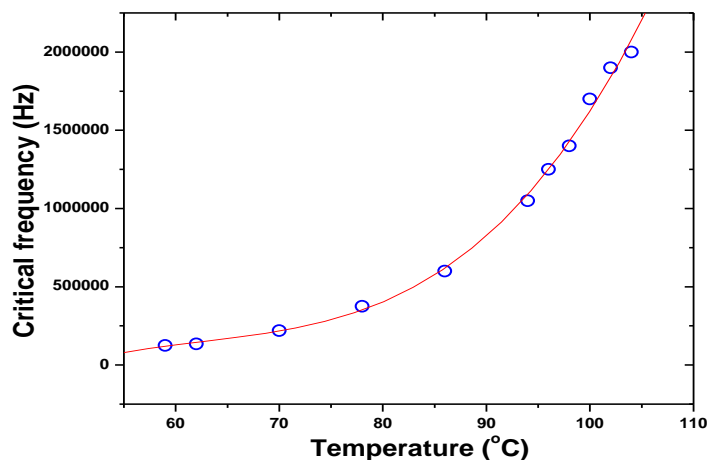
Figure 3.22: Temperature variation of relaxation frequency of compound 4TP-3',3F-4NCS

Reorientations of the entire molecules around their short axis are influenced by smectic and nematic potential barrier which increases with increasing molecular length and decreasing temperature. Relaxation frequency thus increases with temperature and is found to obey Arrhenius law [48,54,55]. From least squares straight line fitting of a plot of ln(τ) versus inverse temperature (Figures 3.23 – 3.25), height of the activation energy barrier of the thermally activated relaxation process was calculated and are listed in Table 3.5. A close look in the values suggests that effect of fluorination and chain length is similar to that of critical frequency.
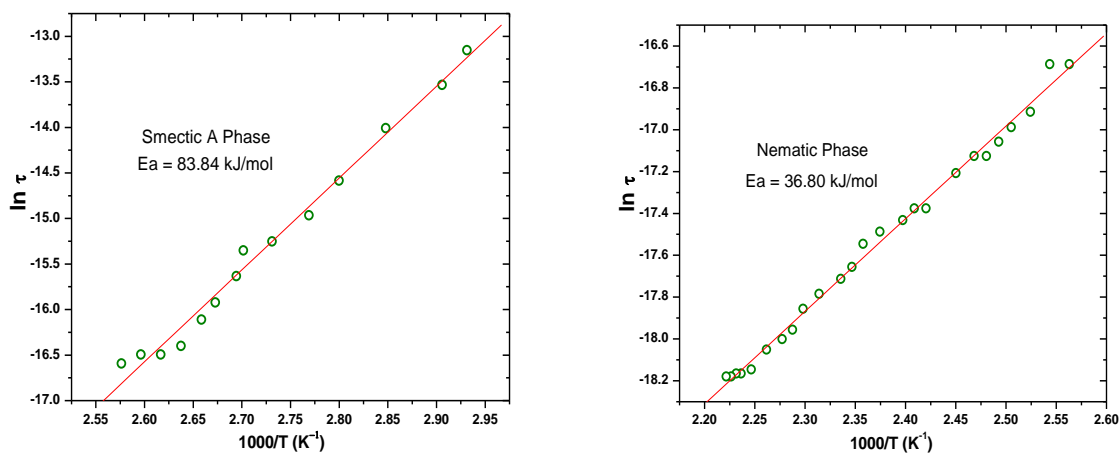
Figure 3.23: Variation of lnτ against 1000/T showing Arrhenius behavior in 2TP-3'F-4NCS.
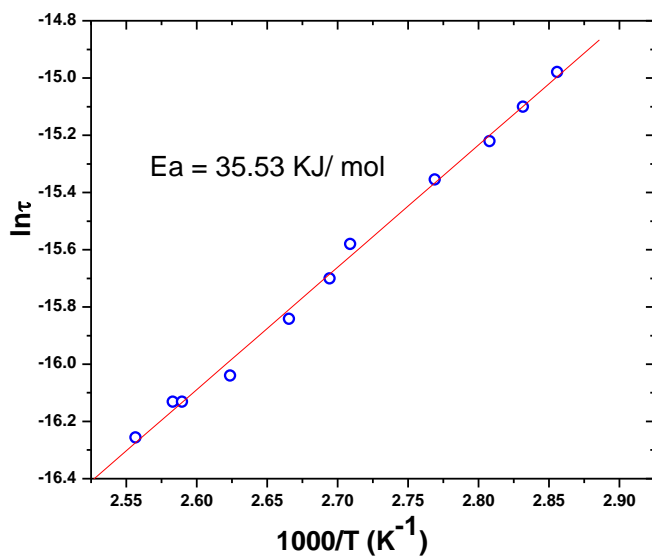
Figure 3.24: Variation of lnτ against 1000/T showing Arrhenius behavior in 2TP-3',3F-4NCS.
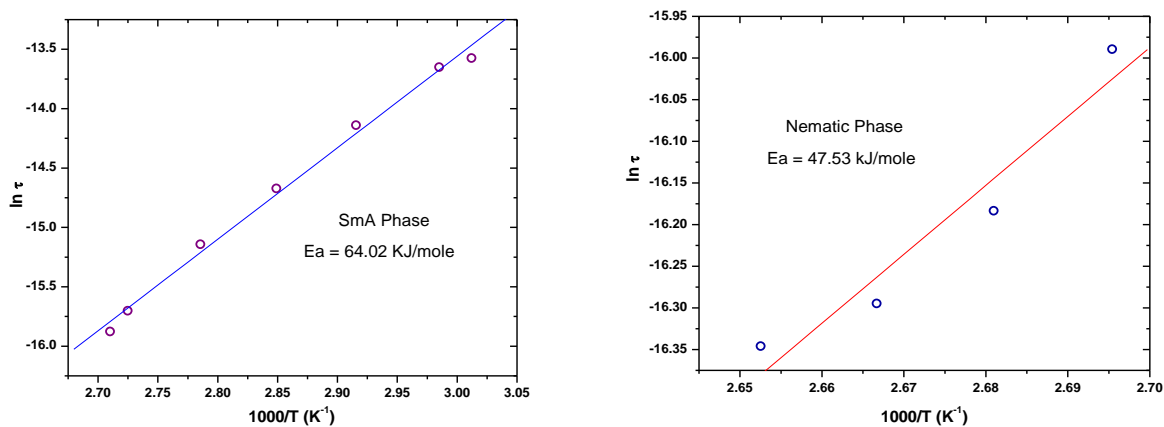
Figure 3.25: Variation of lnτ against 1000/T showing Arrhenius behavior in 4TP-3',3F-4NCS.

Table 3.5: Selected dynamic dielectric parameters of the compounds

Compound	Relaxation Frequency (*fc*)	Activation Energy (kJ/mole)
2TP-3'F-4NCS	82 kHz – 2.5 MHz (SmA) 2.81 MHz – 12.5 MHz (N)	83.8 (SmA) 36.8 (N)
2TP-3',3F-4NCS	510 kHz – 1.77 MHz (N)	35.2 (N)
4TP-3',3F-4NCS	110 kHz to 1.4 MHz (SmA) 1.45 MHz to 2 MHz (N)	64.02 (SmA) 47.53 (N)

3.4.6 Elastic Constants

The splay elastic constant (K_{11}), another important parameter for switching in nematic display devices, were measured using Freédericksz transition method [56]. And their dependence on temperature is shown in Figure 3.26. As K_{11} is proportional to dielectric anisotropy ($\Delta\varepsilon$), it is, as expected, found to exhibit similar decreasing trend with temperature. Near melting point K_{11} in 2TP-3',3F-4NCS is 1.4×10^{-10} N which is almost 1.5 times in 2TP-3'F-4NCS (2.05×10^{-10} N), and almost double (2.67×10^{-10} N) in 4TP-3',3F-4NCS. Thus with increased fluorination splay elastic constant decreases but with increasing chain length it increases. Observed value of K_{11} in 2TP-3',3F-4NCS near Cr-N transition is found to be similar to that observed in non-fluorinated hexylcyclohexyl isothiocyanatobenzene [57] and in singly fluorinated 4-propylphenylbicyclohexyl-3-fluorocyanobenzene but more than that observed in doubly

fluorinated $3PBC^{3,4}F_2$ [44]. Since switching time is inversely proportional to K_{11}, faster response is expected in 4TP-3',3F-4NCS than the ethyl chain based compounds.
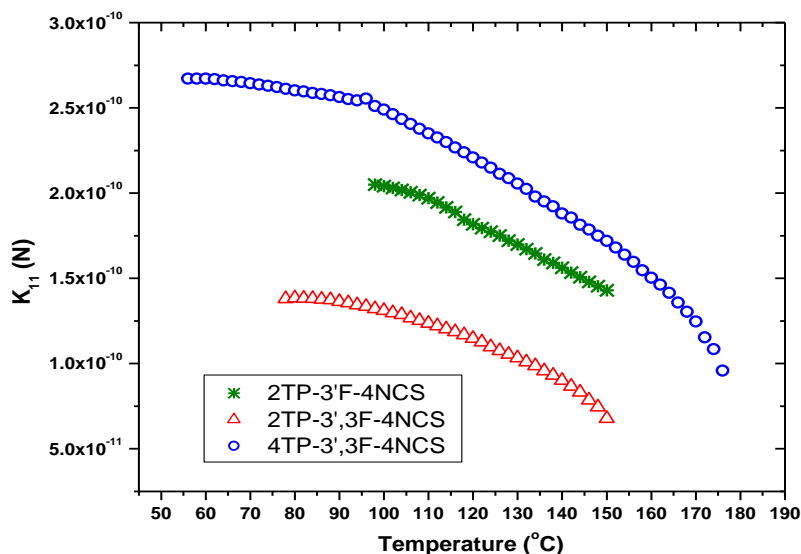
Figure 3.26: Temperature variation of splay elastic constant (K_{11}) of the three compounds.

3.4.7 Optical Birefringence Study

High birefringence (Δn) values are expected for the compounds in question, as the unsaturated rings of the terphenyl structure elongate the π-electron conjugation through the entire rigid core of the molecules and the compounds indeed are found to show high Δn. Selected values of ordinary, extraordinary and average refractive indices (n_o, n_e, n_{av}) and that of optical birefringence (Δn) at some selected temperatures within nematic phase are presented in Table 3.6. Temperature variations of these parameters are shown in Figure 3.27 and Figure 3.28. No measurement was possible in the smectic phase of 2TP-3'F-4NCS and 4TP-3',3F-4NCS. From the figures one can conclude that, although ordinary refractive index is almost the same in 2TP-3'F-4NCS and 2TP-3',3F-4NCS, extraordinary refractive index in 2TP-3',3F-4NCS is found to be less than in 2TP-3'F-4NCS. In 4TP-3',3F-4NCS both n_o and n_e is found to be less compared to the ethyl compounds. Value of n_{avg} also found to decrease with fluorination and increasing chain length. This may be due to less π-electron conjugation along the molecular axis because of

the introduction of additional lateral fluorine atom (laterally substituted fluorine atoms trap π-electrons and pull them away from the conjugation along the main molecular axis) and increased chain flexibility; less order parameter values (discussed below) may also contribute. As expected all the compounds exhibit high birefringence, highest values near melting point being 0.373, 0.357 and 0.333 in 2TP-3'F-4NCS, 2TP-3',3F-4NCS and 4TP-3',3F-4NCS respectively. These values are comparable to reported values in nematic mixtures formulated using isothiocyanato terphenyls or isothiocyanato tolanes [7,21,58]. Although Δn decreases with temperature, it is found to be greater than 0.3 till 164°C in 2TP-3'F-4NCS, 136°C in 2TP-3',3F-4NCS and 130 °C in 4TP-3',3F-4NCS. Commercially available high-Δn TFT-grade *LC* mixtures usually have Δn ~ 0.2 at ambient temperature [59]. Present compounds are therefore expected to be very suitable for formulating high birefringence nematic mixtures, the most suitable will be the singly fluorinated ethyl compound.
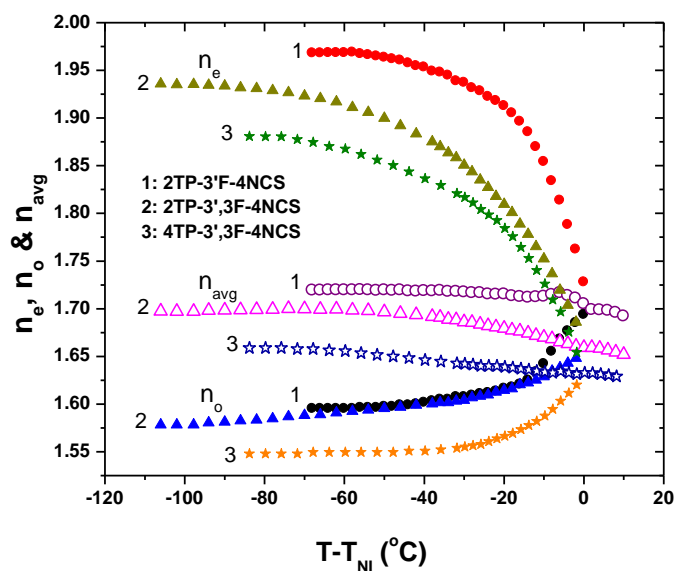
Figure 3.27: Temperature dependence of refractive indices (n_e, n_o, n_{av}) of the three compounds.
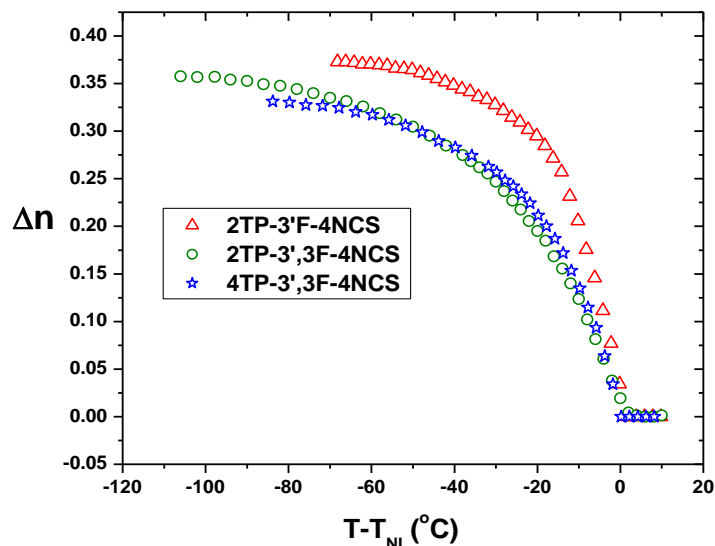
Figure 3.28: Temperature variation of Δn of 2TP-3'F-4NCS, 2TP-3',3F-4NCS and 4TP-3',3F-4NCS.

3.4.8 Density Study

Density values at some selected temperatures are listed in Table 3.6. Variation of density of the compounds with temperature is shown graphically in Figure 3.29. Density is found to decrease strongly with temperature in the ethyl systems. Compared to butyl system singly fluorinated ethyl compound shows stronger temperature dependence than the doubly fluorinated compounds. Because of the second lateral fluorine atom, 2TP-3',3F-4NCS is found to be less densely packed. It is further evident that density increases with chain length (2TP-3',3F-4NCS to 4TP-3',3F-4NCS) but it remains lower than that of 2TP-3'F-4NCS, this may be due to different phase behavior of the molecules.
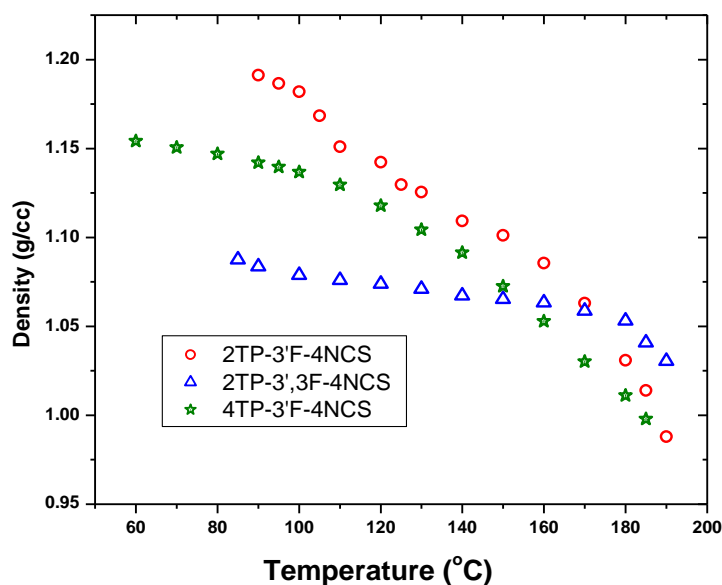
Figure 3.29: Temperature variation of density of 2TP-3'F-4NCS, 2TP-3',3F-4NCS and 4TP-3',3F-4NCS.

Molecular Polarizabilities and Order Prameter

Dependence of calculated principal molecular polarizabilities (α_o, α_e and α_{av}) with temperature is found to be similar to that of the refractive indices. Average value of α is found to be 28.73×10^{-24} cm^3 and 31.04×10^{-24} cm^3 respectively in the singly and doubly fluorinated ethyl compounds. Compound 4TP-3',3F-4NCS possess slightly higher value, α_{av} being 31.25×10^{-24} cm^3. So increased chain length increases α_{av} only marginally but increased fluorination has pronounced effect on α_{av}. Polarizability anisotropy ($\Delta\alpha$) is found to exibit similar decreasing trend with temperature as observed in Δn. From the polarizability values orientational order parameters $<P_2>$ were calculated as described in chapter 2.
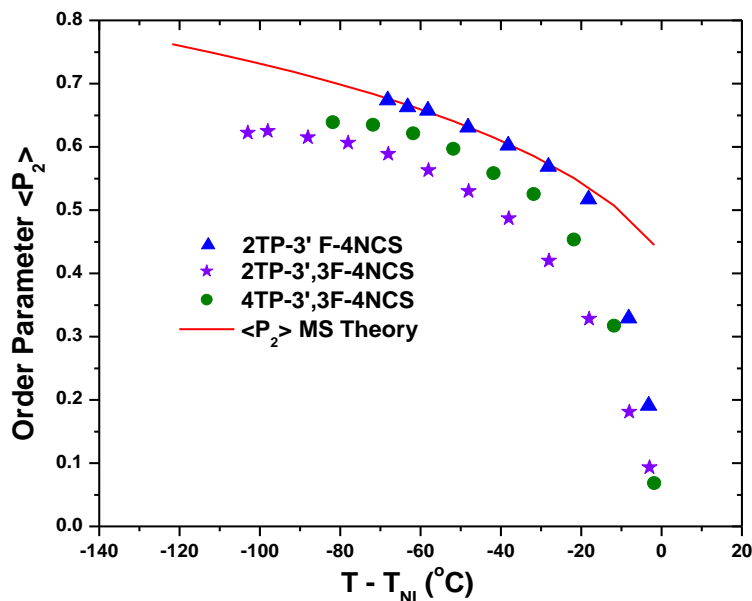
Figure 3.30: Temperature variation of order parameters of 2TP-3'F-4NCS, 2TP-3',3F-4NCS and 4TP-3',3F-4NCS.

The values of polarizability anisotropy ($\Delta\alpha$) and order parameters $<P_2>$ at some selected temperatures for the three compounds are listed in Table 3.6. Temperatre variation of $<P_2>$ is depicted graphically in Figure 3.30. Order parameters computed on the basis of Maier-Saupe (MS) mean field theory for calamitic nematogens have also been depicted in the same figure. As expected, order parameter is more in smectic phase than in nematic phase in 2TP-3'F-4NCS and 4TP-3',3F-4NCS. Order parameter of the singly fluorinated ethyl compound is substantially more than the doubly fluorinated ones. Thus the doubly fluorinated ethyl compound is not only less densely packed but orientationally less ordered as well. Order parameter of 4TP-3',3F-4NCS lies between the two ethyl compounds. Thus combined effect of increased chain flexibility and lateral fluorination on order parameter is less than only lateral fluorination. Moreover, only in the singly fluorinated ethyl compound $<P_2>$ values match nicely with MS theoretical values, while in the other two compounds these are considerably less. Such behavior has been reported earlier [60-62]. However, no discontinuity is observed at transitions in refractive indices, densities and order parameters as seen in dielectric and structural parameters.

Table 3.6: Selected refractive indices (n_e & n_o), optical birefringence (Δn), density (ρ), polarizability anisotropy ($\Delta\alpha$) and order parameter $<P_2>$

Compound	Temp (°C)	n_e	n_o	Δn	ρ (g/cc)	$\Delta\alpha$	$<P_2>$
2TP-3'F-4NCS	120	1.969	1.596	0.373	1.142	20.500	0.674
	125	1.969	1.596	0.373	1.129	20.165	0.663
	130	1.969	1.596	0.373	1.126	20.009	0.658
	140	1.963	1.598	0.365	1.109	19.197	0.631
	150	1.949	1.604	0.345	1.101	18.328	0.602
2TP-3',3F-4NCS	85	1.935	1.578	0.357	1.087	20.388	0.622
	90	1.935	1.578	0.357	1.084	20.473	0.625
	100	1.932	1.582	0.350	1.079	20.138	0.615
	110	1.929	1.585	0.344	1.076	19.860	0.606
	120	1.922	1.588	0.334	1.074	19.279	0.589
	130	1.911	1.592	0.319	1.071	18.445	0.563
	140	1.895	1.596	0.299	1.067	17.361	0.530
	150	1.875	1.600	0.275	1.065	15.949	0.487
4TP-3',3F-4NCS	100	1.881	1.548	0.333	1.137	20.228	0.639
	110	1.877	1.548	0.329	1.129	20.161	0.635
	120	1.870	1.549	0.321	1.118	19.833	0.621
	140	1.836	1.551	0.285	1.091	18.053	0.558
	160	1.793	1.564	0.229	1.053	14.956	0.454
	170	1.740	1.582	0.158	1.030	10.507	0.317

3.5 CONCLUSION

Effect of lateral fluorination and increased chain length on several physical parameters, important from application consideration, of three compounds 2TP-3'F-4NCS, 2TP-3',3F-4NCS and 4TP-3',3F-4NCS having terphenyl rigid core structures with terminal isothiocyanate (NCS) polar groups has been investigated. The first and the third compound possess smectic phase as well as nematic phase while the second compound possess only nematic phase. All the three compounds exhibit very broad range nematic phase viz., 68°C, 108°C and 85°C respectively. Molecular mechanics calculation revealed that the molecules possess a strong axial dipole moment of 5.57D, 6.68D and 6.29D respectively. From optimized geometry the calculated length of the molecules are found to be 18.56 Å, 18.05 Å and 20.82 Å respectively which are slightly less than that obtained from X-Ray diffraction study. This suggests, contrary to common perception that NCS molecules do not form dimers, presence of weak antiparallel correlation of molecules in all the three compounds. Calculated effective values of dipole moments in mesophases and dipole-dipole correlation factors support this observation. Observed dielectric anisotropy is positive in all the three compounds and strong enough to ensure a driving voltage suitable for thin TFT based LC display cell. Calculated splay elastic constants suggest that the singly fluorinated compound (2TP-3'F-4NCS) will exhibit faster response than the other two doubly fluorinated compounds. Only one relaxation process with strong absorption, related with rotation around short molecular axis, is observed, critical frequency of which is found to decrease with increased fluorination and chain length. The singly fluorinated compound is found to exclude the possibility of undesirable energy absorption below MHz range applications. Nature of the absorption process is found to be almost Debye type in all the systems. Above all the compounds exhibit high birefringence, highest values being 0.373, 0.357 and 0.333 respectively. Thus with increasing fluorination and increasing chain length the birefringence gradually decreases. Combined effect of increased chain flexibility and lateral fluorination on order parameter is less than only lateral fluorination. These compounds are, therefore, expected to be very suitable for formulating high birefringence nematic mixtures for fast switching displays.

3.6 REFERENCES

[1] S. Gauza, H. Wang, C. H. Wen, S. T. Wu, A. Seed and R. Dabrowski; Jpn. J. Appl. Phys., 42, 3463 (2003), High Birefringence Isothiocyanato Tolane Liquid Crystals.

[2] J. S. Gasowska, S. J. Cowling, M. C. R. Cockett, M. Hird, R. A. Lewis, E. P. Raynes and J. W. Goodby; J. Mater. Chem., 20, 299 (2010), The influence of an alkenyl terminal group on the mesomorphic behaviour and electro-optic properties of fluorinated terphenyl liquid crystals.

[3] A. Mori, M. Hashimoto and S. Ujiiec; Liq. Cryst., 38, 263 (2011), Effects of a semi-fluorinated side chain and a lateral polar group on mesomorphic properties of 5-cyanotroponoids and benzonitriles.

[4] D. Demus, Y. Goto, S. Swada, E. Nakagawa, H. Saito and R. Tarao; Mol. Cryst. Liq.Cryst., 260, 1 (1995), Trifluorinated Liquid Crystals for TFT Displays.

[5] T. Nishi, A. Matsubara, H. Okada, H. Onnagawa, S. Sugimori, and K. Miyashita; Jpn. J. Appl. Phys., 34, 236 (1995), Relationship between Molecular Structure and Temperature Dependence of Threshold Voltage in Fluorinated Liquid Crystals.

[6] V. F. Petrov; Liq. Cryst., 19, 729 (1995), Liquid crystals for AMLCD and TFT-PDLCD applications.

[7] S. Gauza, X. Zhu, W. Piecek, R. Dabrowski, S. T. Wu; J. Disp. Technol. 3 (3), 250-252 (2007), Fast Switching Liquid Crystals for Color-Sequential LCDs.

[8] M. Schadt, W. Helfrich; Appl. Phys. Lett., 18, 127 (1971), Voltage-dependent optical activity of a twisted nematic liquid crystal.

[9] K. Nishiyama, M. Okita, S. Kawaguchi, K. Teranishi, R. Takamatsu; SID Tech. Dig. 36, 132 (2005), 32″ WXGA LCD TV using OCB Mode, Low Temperature p-Si TFT and Blinking Backlight Technology.

[10] G. Harbers, C. Hoelen, SID Tech. Dig; 32, 702 (2001), High Performance LCD Back lighting using High Intensity Red, Green and Blue Light Emitting Diodes.

[11] D. P. Resler, D. S. Hobbs, R. C. Sharp, L. J. Friedman, T.A. Dorschner; Opt. Lett. 21 (9), 689 (1996), High-efficiency liquid-crystal optical phased-array beam steering.

[12] J. Y. Hardeberg, F. Schmitt, H. Brettel; Opt. Eng. 41 (10), 2532 (2002), Multispectral color image capture using a liquid crystal tunable filter.

[13] H. C. Lin, Y. H. Lin; Opt. Express, 20 (3), 2045 (2012), An electrically tunable-focusing liquid crystal lens with a low voltage and simple electrodes.

[14] T.T. Ru, C.C. Yuan, R.P. Pan, C.L. Pan, X.C. Zhang; IEEE Microwave Wireless Compon. Lett. 14 (2) (2004), Electrically controlled room temperature terahertz phase shifter with liquid crystal.

[15] R. L. Sutherland, V. P. Tondiglia, L.V. Natarajan; Appl. Phys. Lett. 64, 1074 (1994), Electrically switchable volume gratings in polymer-dispersed liquid crystals.

[16] N. Mizoshita, K. Hanabusa, T. Kato; Adv. Funct. Mater. 13, 313 (2003), Fast and High-Contrast Electro-optical Switching of Liquid-Crystalline Physical Gels: Formation of Oriented Microphase-Separated Structures.

[17] Y. H. Fan, H. W. Ren, S. T. Wu; Appl. Phys. Lett. 82, 2945 (2003), Normal-mode anisotropic liquid-crystal gels.

[18] M. Hird; Chem. Soc. Rev., 2007; 36, 2070, Fluorinated liquid crystals − properties and applications.

[19] J. A. Malecki and J. Nowak; J. Molecular Liquids, vol. 81, 245-252 (1999), Intermolecular interactions in benzene solutions of 4-heptyl-3'-cyano-biphenyl studied with non-linear dielectric effects.

[20] S. Gauza, J. Li, S. T. Wu, A. Spadlo, R. Dabrowski, Y. N. Tzeng, K. L. Cheng, Liq. Cryst. 32(8), 1077 (2005), High birefringence and high resistivity isothiocyanate-based nematic liquid crystal mixtures.

[21] S. Gauza, S. T. Wu, A. Spadło, R. Dabrowski, J. Disp.Technol. 2(3), 247 (2006), High performance room temperature nematic liquid crystals based on laterally fluorinated isothiocyanato-tolanes.

[22] D. Sinha, D. Goswami, P. K. Mandal, Ł. Szczucinski, R. Dabrowski; Mol Cryst Liq Cryst., 562,156 (2012), On the nature of molecular associations, static permittivity and dielectric relaxation in a uniaxial nematic liquid crystal.

[23] B. Jha, S. Paul, R. Paul, P. Mandal; Phase Transitions, 15, 39 (1989), Order parameters of some homologue cybotactic nematics from X-ray diffraction measurements.

[24] A. de Vries; Mol Cryst Liq Cryst., 10, 31 (1970), Evidence for the existence of more than one type of nematic phase.

[25] B. R. Jaishi, P. K. Mandal; Liq Cryst., 33, 753 (2006), Optical microscopy, DSC and X-ray diffraction studies in binary mixtures of 4-pentyloxy-49-cyanobiphenyl with three 4,49-di(alkoxy) azoxybenzenes.

[26] P.G. de Gennes; Mol. Cryst. Liq. Cryst., 12, 193 (1971), Short range order effects in the isotropic phase of nematics and cholesterics.

[27] H. E. J. Neugebauer; Canad. J. Phys., 32, 1-8 (1954), Clasius-Mossoti equation for certain types of anisotropic crystals.

[28] Hyperchem 6.03, Hypercube Inc., Gainesville, FL, USA.

[29] S. Biswas, S. Haldar, P. K. Mandal, K. Goubitz, H. Schenk and R. Dabrowski, Crystal Research and Technology, Vol. 42, No.10, P. 1029 − 1035 (2007), Crystal structure of a polar nematogen 4-(trans-4-undecylcyclohexyl) isothiocyanatobenzene.

[30] E. Megnassan and A. Proutierre; Mol. Cryst. Liq. Cryst., 108, 245-254 (1984), Dipole Moments and Kerr Constants of 4-n-Alkyl-4'-Cyanobiphenyl Molecules (From 1CB to 12CB) Measured in Cyclohexane Solutions.

[31] P. Sarkar, P. Mandal, S. Paul, R. Paul; Liq. Cryst, Vol. 30, No. 4, 507–527 (2003), X-ray diffraction, optical birefringence, dielectric and phase transition properties of the long homologous series of nematogens 4-(trans-4'-n-alkylcyclohexyl) isothiocyanatobenzenes.

[32] A de Vries; Mol Cryst Liq Cryst., 10, 219 (1970), X-ray photographic studies of liquid crystals I. A cybotactic nematic phase.

[33] P. Sarkar, P. Mandal, S. Paul, R. Dabrowski, K. Czuprynski; Liq.Cryst. 30 (4), 507 (2003), X-ray diffraction, optical birefringence, dielectric and phase transition properties of the long homologous series of nematogens 4-(trans -4′- n -alkylcyclohexyl) isothiocyanatobenzenes.

[34] S. Haldar, S. Barman, P. K. Mandal, W. Haase, R. Dabrowski; Mol. Cryst. Liq.Cryst., 528, 81-95 (2010), Influence of Molecular Core Structure and Chain Length on the Physical Properties of Nematogenic Fluorobenzene Derivatives.

[35] W. L. McMillan; Phys. Rev A, 4, 1238-1246 (1971), Simple molecular model for the smectic A phase of liquid crystals.

[36] W. L. McMillan; Phys. Rev A, 6, 936 (1972), X-Ray Scattering from Liquid Crystals. I. Cholesteryl Nonanoate and Myristate.

[37] P. Sarkar, P. Mandal, S. Paul, R. Dabrowski, K. Czuprynski; Liq Cryst. 30 (4), 507 (2003), X-ray diffraction, optical birefringence, dielectric and phase transition properties of the long homologous series of nematogens 4-(trans-4∞-n-alkylcyclohexyl)isothiocyanatobenzenes.

[38] A. J. Leadbetter, R. M. Richardson, C. N. Cooling; J Phys (Paris), 36 (C1), 37 (1975), The structure of a number of nematogens.

[39] P. K. Sarkar, S. Paul, P. Mandal; Mol Cryst Liq Cryst., 265, 249 (1995), Small angle X-ray scattering studies on smectic and nematic phases of a toluidine compound.

[40] N. V. Madhusudana, S. Chandrasekhar; Pramana Suppl., 1, 57 (1975), The role of permanent dipoles in nematic order.

[41] S. Haldar, S. Biswas, P. K. Mandal, K. Goubitz, H. Schenk and W. Haase; Mol. Cryst. Liq. Cryst., 490, 80-87 (2008), X-Ray Structural Analysis in the Crystalline Phase of a Nematogenic Fluoro-Phenyl Compound.

[42] S. Haldar, P. K. Mandal, S.J. Prathap, T. N. Guru Row and W. Haase; Liq. Cryst., 35, 1307-1312 (2008), X-ray studies of the crystalline and nematic phases of 49-(3,4,5-trifluorophenyl)-4-propylbicyclohexyl.

[43] S. Biswas, S. Haldar, P. K. Mandal, K. Goubitz, H. Schenk, R. Dabrowski; Crystal Res Technol., 42(10), 1029-1035 (2007), Crystal structure of a polar nematogen 4-(trans-4-undecylcyclohexyl) isothiocyanatobenzene.

[44] H. Ishikawa, A. Toda, H. okada, H. Onnagawa, S. Sugimori; Liq. Cryst., 22, 743 (1997), Relationship between order parameter and physical constants in fluorinated liquid crystals.

[45] S. Urban, P. Kula, A. Spadlo, M. Geppi, A. Marini; Liq.Cryst., 37, 1321 (2010), Dielectric properties of selected laterally fluoro-substituted 4,4″-dialkyl, dialkoxy and alkyl-alkoxy [1:1′;4′:1″] terphenyls.

[46] P. Bordewijk, Physica, 75, 146 (1974), Extension of the Kirkwood-Frölich Theory of the Static dielectric Permittivity to anisotropic Liquids.

[47] N. V. Madhsudana, B. S. Srikanta, R. Subramanya, M. Urs, Mol. Cryst. Liq. Cryst. 108, 19 (1984), Comparative X-ray and dielectric studies on some structurally related smectogenic compounds.

[48] J. Schacht, P. Zugenmaier, M. Buivydas, L. Komitov, B. Stebler, S. T. Lagerwall, F. Gouda, F. Horii; Phys Rev E., 61, 3926 (2000), Intermolecular and intramolecular reorientations in nonchiral smectic liquid-crystalline phases studied by broadband dielectric spectroscopy.

[49] S. Urban, R. Dabrowski, J. Dziaduszek, J. Janik, J. K. Moscicki; Liq. Cryst. 26, 1817 (1999), Mesomorphic and dielectric properties of fluorosubstituted isothiocyanates with different bridging groups.

[50] L. Benguigui; Phys. Rev. A, 28, 1852 (1983), Dielectric relaxation in the crystalline smectic-B phase.

[51] M. Gu, Y. Yin, S. V. Shiyanovskii, O. D. Lavrentovich; Phys Rev E., 76, 061702 (2007), Effects of dielectric relaxation on the director dynamics of uniaxial nematic liquid crystals.

[52] H. Baessler, R. B. Beard, M. M. Labes; J Chem Phys., 52, 2292 (1970), Dipole Relaxation in a Liquid Crystal.

[53] J. Czub, R. Dabrowski, J. Dziaduszek, S. Urban; Phase Transition, 82, 485-495 (2009), Dielectric properties of ten three-ring LC fluorosubstituted isothiocyanates with different mesogenic cores.

[54] A. C. Diogo, A. F. Martins; J Phys (Paris)., 43, 779 (1982), Order parameter and temperature dependence of the hydrodynamic viscosities of nematic liquid crystals.

[55] S. Arrhenius; Z Phys Chem., 4, 226 (1889), On the reaction rate of the inversion of non-refined sugar upon souring.

[56] B. Kundu, S. K. Pal, S. Kumar, R. Pratibha, N. V. Madhusudana; Physical Review E., 82, 061703 (2010), Splay and bend elastic constants in the nematic phase of some disulfide bridged dimeric compounds.

[57] R. Dhar, A. S. Pandey, M. B. Pandey, S. Kumar and R. Dabrowski; Applied Physics Express 1, 121501 (2008), Optimization of the display parameters of a room temperature twisted nematic display material by doping single-wall carbon nanotubes.

[58] M. D. Gupta, A. Mukhopadhyay, S. K. Roy, R. Dabrowski; J Appl Phys., 113, 053516 (2013), High birefringence liquid crystal mixtures: Optical properties and order parameter.

[59] E. Nowinowski-Kruszelnicki, J. Kedzierski, Z. Raszewski, L. Jaroszewicz, R. Dabrowski, M. Kojdecki, W. Piecek, P. Perkowski, K. Garbat, M. Olifierczuk, M. Sutkowski, Karolina Ogrodnik, P. Morawiak, E. Miszczyk; Optica Applicata, Vol. XLII, No. 1, oa120116 (2012), High birefringence liquid crystal mixtures for electro-optical devices.

[60] H. S. Subramhanyam, C. S. Prabha and D. Krishnamurti; Mol. Cryst. Liq. Cryst., 28, 201 (1974), Optical Anisotropy of Nematic Compounds.

[61] M. Mitra, S. Paul and R. Paul; Pramäna J. Phys., 29, 409 (1987), Optical Birefringence and Order Parameter of Three Nematogens.

[62] N. V. Madhusudana, Mol. Cryst. Liq. Cryst., 59, 117 (1980), Polarization Field and Orientational Order in Liquid Crystals.